RESEARCH PAPER

Islets 6:5-6, e995997; September–December 2014; © 2014 Taylor & Francis Group, LLC

Impact of exposure to low concentrations of nitric oxide on protein profile in murine and human pancreatic islet cells

Rafael Tapia-Limonchi[1], Irene Díaz[1], Gladys M Cahuana[1], Mario Bautista[1], Franz Martín[1], Bernat Soria[2], Juan R Tejedo[1], and Francisco J Bedoya[1,*]

[1]Andalusian Center for Molecular Biology and Regenerative Medicine (CABIMER)- Pablo de Olavide University; Biomedical Research Network (CIBER) of Diabetes and Related Metabolic Diseases; RED-TERCEL; Seville, Spain; [2]Andalusian Center for Molecular Biology and Regenerative Medicine (CABIMER)-Fundación Progreso y Salud; Biomedical Research Network (CIBER) of Diabetes and Related Metabolic Diseases; RED-TERCEL; Seville, Spain

Keywords: pancreatic β cell, protein profile, nitric oxide, islet survival

Homeostatic levels of nitric oxide (NO) protect efficiently against apoptotic death in both human and rodent pancreatic β cells, but the protein profile of this action remains to be determined. We have applied a 2 dimensional LC-MS-MALDI-TOF/TOF-based analysis to study the impact of protective NO in rat insulin-producing RINm5F cell line and in mouse and human pancreatic islets (HPI) exposed to serum deprivation condition. 24 proteins in RINm5F and 22 in HPI were identified to undergo changes in at least one experimental condition. These include stress response mitochondrial proteins (UQCRC2, VDAC1, ATP5C1, ATP5A1) in RINm5F cells and stress response endoplasmic reticulum proteins (HSPA5, PDIA6, VCP, GANAB) in HPI. In addition, metabolic and structural proteins, oxidoreductases and chaperones related with protein metabolism are also regulated by NO treatment. Network analysis of differentially expressed proteins shows their interaction in glucocorticoid receptor and NRF2-mediated oxidative stress response pathways and eNOS signaling. The results indicate that exposure to exogenous NO counteracts the impact of serum deprivation on pancreatic β cell proteome. Species differences in the proteins involved are apparent.

Introduction

Diabetes mellitus is characterized by the loss of pancreatic β cell ability to respond to stressful conditions and proteomic studies have provided substantial evidence on the process.[1-6] Thus, exposure to inflammatory cytokines alters the expression of 19 proteins of a total of 1600 detectable proteins in rat islets.[1] The actions of this mediators of the inflammatory response are mediated at least in part by the generation of micromolar amounts of NO.[7,8] Although damage to mitochondria and DNA is involved in the process of NO-induced β cell death, additional evidence indicates that the ER stress pathway is also implied.[9] By contrast, protective actions of both insulin and IGF-1 in both rodent and human pancreatic β cells involve the generation of homeostatic NO and the activation of the c-Src PI3K/Akt anti-apoptotic pathway in a Pdx1-dependent manner.[10-12] Despite the documented role of NO in the survival response in insulin producing β cells, a comprehensive account of the molecular process involved remains to be pictured. This study aimed to characterizing at the protein level protective action of NO against stress induced by serum deprivation in both rodent and human islet cells. The results reported here shows that homeostatic concentrations of NO regulates the expression of chaperones, peroxiredoxins, disulphide isomerases and proteins involved in the mitochondrial and endoplasmic reticulum response to stress. A group of proteins targeted by the transcription factor NRF2 was identified, thus suggesting that this factor might be involved in regulation of the response against stress in β cells.

Results

Differential proteomic profile of nitric oxide-exposed RINm5F cells

To investigate changes in protein profile of RINm5F cells exposed to serum deprivation and the effect of the NO donor DETA/NO, 2-D gel electrophoresis was performed in 3 biological replicates of cells cultured in the presence of serum (+ serum), absence of serum (- serum), and absence of serum supplemented with 10 μM DETA/NO (- serum + DETA/NO). Image analysis of gels was performed by BioRad PDQuest 7.4 software and includes manual editing of artifacts and speckles. One gel was determined as the master gel and background was removed from each gel accordingly. 417 spots were detected in the reference gel (**Fig. 1**). Comparison of the 9 gels showed that the most abundant and visible spots were present in all gels. To elucidate

*Correspondence to: Francisco J Bedoya; Email: francisco.bedoya@cabimer.es
Submitted: 06/20/2014; Revised: 10/23/2014; Accepted: 12/04/2014
http://dx.doi.org/10.1080/19382014.2014.995997

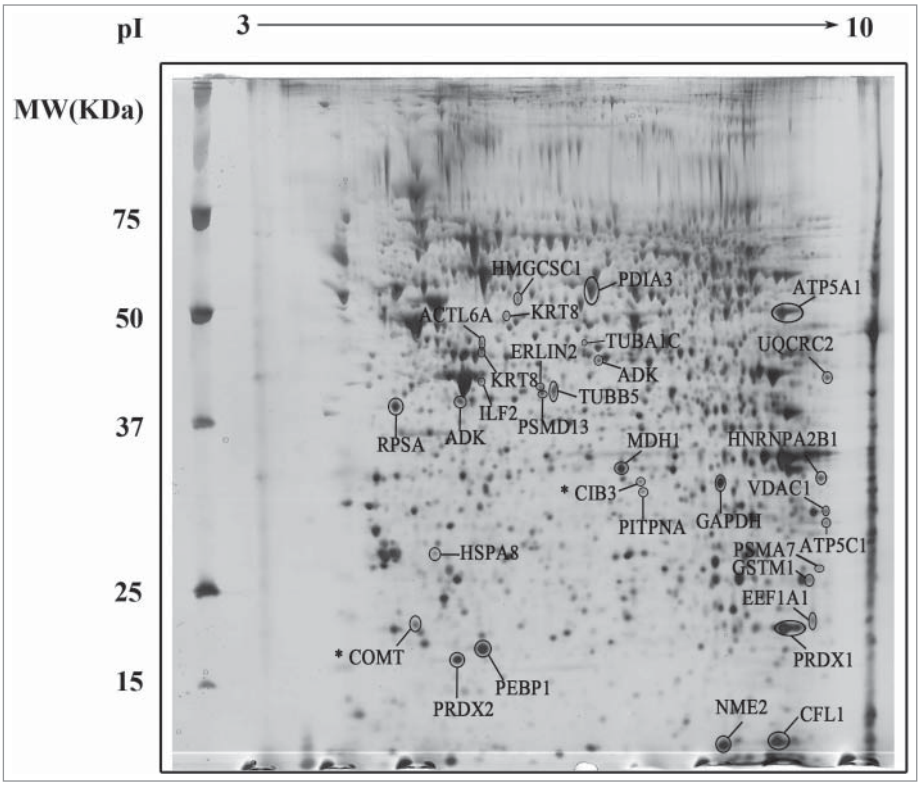

Figure 1. Representative 2-D gel map of RINm5F cells. Protein extracts were loaded onto an IPG strip (pH 3 – 10) and subsequently separated by molecular weight in a 12% SDS-PAGE. Gels were stained by MS-compatible silver nitrate staining. The spots were analyzed by MS-MALDI-TOF/TOF. Spots for differentially expressed proteins are indicated. * Indicates proteins with a Mascot Protein Score for identity less than 71.

changes among the culture conditions, an image analysis using PD Quest 7.4 software was performed as described in Materials and Methods, for selecting differentially expressed proteins. The analysis resulted in a set of 32 differentially expressed proteins when compared to the control condition (+ serum). These proteins were characterized by MALDI-TOF/TOF-MS peptide mass fingerprinting and database searching using the MASCOT program. The criteria used to accept identifications included the number of peptides matched and the probability that the observed match is a random event expressed as −10LogP (protein score) where scores greater than 71 are significant ($p<0.05$). The characterized proteins are listed in **Table 1**. Two spots (21 and 24) had no significant identification protein score. A third spot (spot 4) does not match with the corresponding mobility in the gel.

Among the 29 identified proteins, 24 are differentially expressed in at least in one condition and 5 (ILF2, HNRNPA2B1, ATP5A1, PDIA3 and MDH1) exhibit minor changes in – serum and - serum + DETA/NO conditions. Treatment with NO leads to decreased expression of 14 proteins and increased expression of 7 (**Fig. 2A**). 3 proteins do not change with NO treatment (HSP90AB1 and CFL1 increased and PRDX2 decreased during culture in – serum condition). The functional categories, sub-cellular localization, protein functions and network enrichment of identified proteins were assessed and generated using Ingenuity Pathway Analysis software (Ingenuity® Systems, www.ingenuity.com). GO analysis revealed that 18 differentially expressed proteins are involved in 7 top functional categories having a –log (p-value) higher than 3, including small molecule biochemistry, cell death/survival, molecular transport, cell growth proliferation, free radical scavenging, DNA replication recombination repair, and energy production (**Fig. 2B**). When analyzing cellular localization, the highest proportion of proteins were located in cytoplasm (34%) and in cytoplasm/nucleus (24%), whereas remaining proteins are located in mitochondria (14%), membrane/cytoplasm (14%), endoplasmic reticulum (7%) and nucleus (7%) (**Fig. 2C**). Identified proteins were also categorized according to the function by using the annotations in the Swiss-Prot database; 15% are metabolic proteins, 15% are structural proteins, 5 10% fractions correspond to proteins involved in ion transport, chaperones related with protein metabolism, oxidoreductases, gene expression and proteins components of the proteasome, 7% are chaperones related with RNA processing, 3% are proteins of the electron transport chain and 10% correspond to other proteins (**Fig. 2D**).

Differential proteomic profile of nitric oxide-exposed human and mouse pancreatic islets

Human islets were stabilized by culture in suspension for 3 days in the presence of serum. Then, batches of islets were exposed for 19 h to 3 experimental conditions: control, serum (+ serum), serum deprivation (- serum), serum deprivation +10 μM DETA/NO (- serum + DETA/NO). 110 spots were detected in the reference gel (**Fig. 3**). Comparison of the 9 gels showed that the most abundant and visible spots were present in all gels. To elucidate changes among the culture conditions, an image analysis using PD Quest 7.4 software was performed as described in Materials and Methods, for selecting differentially expressed proteins. The analysis resulted in a set of 29 proteins that are differentially expressed when compared with the control condition (+ serum). These proteins were identified according to the criteria used with RINm5F cells and listed in **Table 2**. Spots 1, 8 13 and 21 had no significant identification protein score. 22 proteins were differentially expressed in at least one condition and 3 (ALDH1A1, HNRNPH1 and PDIA3) show a minor change in – serum and - serum + DETA/NO conditions. NO treatment decreased the expression of 10 proteins and increased the expression of 7 proteins. 5 proteins do not change with the NO treatment (GANAB, VCP and HSPA5 decreased, while

Table 1. Identification of proteins differentially expressed after treatment with 10μM of DETA/NO in absence of serum in RINm5F rat insulinoma cells.

Spot ID	Official symbol	Name	Protein MW/PI	No. peptides identified MASCOT	Mascot Protein Score	Biological Process
1	HMGCS1	3-hydroxy-3-methylglutaryl-Coenzyme A synthase 1	58024,7/5,58	21	295	Metabolism
2	KRT8	Keratin 8	53985,3/5,83	26	389	Cell Proliferation
3	ACTL6A	Actin-like 6A	47903,5/5,39	14	191	Cell Proliferation
4	KRT8	Keratin 8	53985,3/5,83	25	400	Cell Proliferation
5	TUBA1C	Tubulin α 1C	49937,3/ 4.96	11	171	Cell Proliferation
6	ADK	Adenosine kinase	40449,4/5,84	10	137	Cell Proliferation
7	ILF2	Interleukin enhancer binding factor2	51474,6/5,42	11	73	Cell Death and Survival
8	HSP90AB1	Heat shock protein 90 α (cytosolic), class B member 1	83572,2/4,95	15	229	Cell Death and Survival
9	ERLIN2	ER lipid raft associated 2	37710.3/5,54	14	273	Metabolism
10	PSMD13	Proteasome (prosome, macropain) 26S subunit, non-ATPase, 13	43075,3/5,55	24	393	Cell Death and Survival
11	TUBB5	Tubulin, β 5 class I	50095,1/4,78	23	468	Cell Proliferation
12	UQCRC2	Ubiquinol cytochrome c reductase core protein 2	48423,2/9,16	12	146	Cell Death and Survival
13	HNRNPA2B1	Heterogeneous nuclear ribonucleoproteins A2/B1	37511,8/8,97	23	545	Cell Death and Survival
14	VDAC1	Voltage-dependent anion channel 1	32060,2/8,35	12	228	Cell Death and Survival
15	ATP5C1	ATP synthase, H^+ transporting, mitochondrial F1 complex, gamma polypeptide 1	30228,7/8,87	9	104	Cell Death and Survival
16	PSMA7	Proteasome (prosome, macropain) subunit, α type 7	28009,7/8,6	13	178	Cell Death and Survival
17	PRDX1	Peroxiredoxin-1	22323,4/8,27	12	352	[a]Cell Death and Survival
18	EEF1A1	Eukaryotic translation elongation factor 1 α 1	50113.8/9,29	8	163	Metabolism
19	HSPA8	Heat shock protein 8	70871.07/5.37	10	176	Cell Death and Survival
20	GAPDH	Glyceraldehyde-3-phosphate dehydrogenase	36090,1/8,14	14	386	Metabolism
21	CIB3	Calcium and integrin-binding family member 3	22057.9/4.56	8	66 *	Metabolism
22	PITPNA	Phosphatidylinositol transfer protein, α	31907.4/5.96	11	138	Metabolism
23	GSTM1	Glutathione S-transferase Mu1	25937,1/8,42	25	561	Cell Death and Survival
24	COMT	Catechol O-methyltransferase	24959,5/5,11	6	64 *	Metabolism
25	PRDX2	Peroxiredoxin-2	21783.6/5.34	10	260	[a]Cell Death and Survival
26	PEBP1	Phosphatidylethanolamine-binding protein 1	20902,4/5,48	12	419	Cell Death and Survival
27	NME2	NME/NM23 nucleoside diphosphate kinase 2	17385,9/6,92	15	451	Metabolism
28	CFL1	Cofilin 1, non-muscle	18748,8/8,22	10	202	Cell Proliferation
29	RPSA	Ribosomal protein SA	32824.05/4,80	15	599	Cell Proliferation
30	PDIA3	Protein disulfide isomerase associated 3	57009,9/5,88	34	616	Cell Death and Survival
31	MDH1	Malate dehydrogenase 1, NAD (soluble)	36632,1/5,93	13	380	Metabolism
32	ATP5A1	ATP synthase, H^+ transporting, mitochondrial F1 complex, α subunit 1	59830,7/9,22	26	587	[a]Cell Death and Survival

*Protein score is −10*Log(P), where P is the probability that the observed match is a random event. Protein scores greater than 71 are significant ($p<0.05$).
[a]Involved in β-cell survival

P4HB and PDIA6 increased during culture in – serum condition) (**Fig. 4A**). As above, GO analysis revealed that 18 differentially expressed proteins are involved in 8 functional categories having a –log (p-value) higher than 3 (**Fig. 4B**). The categories are: post translational modification, protein folding, DNA replication recombination repair, energy production, small molecule biochemistry, cell death/survival, cell growth and proliferation and cellular compromise. Cellular distribution of proteins was: cytoplasmic (52%), endoplasmic reticulum (20%), nucleus (12%), mitochondrion (8%), cell membrane (4%) and

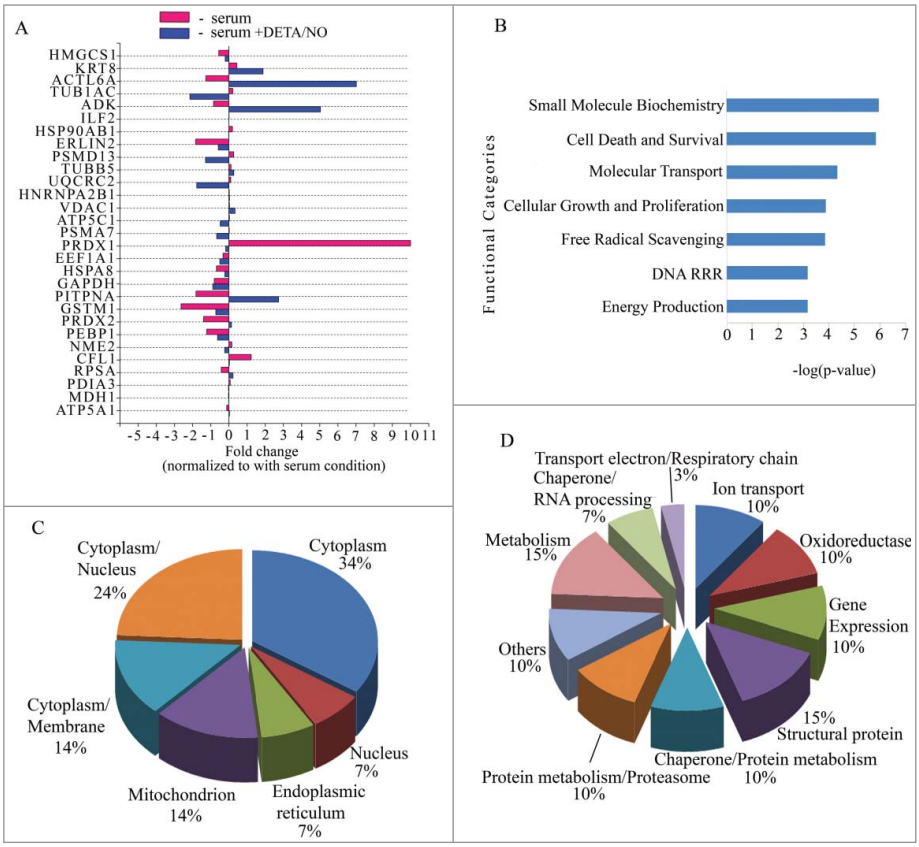

Figure 2. Characterization of differentially expressed proteins in RINm5F cells (**A**) Bar graph of the fold changes for differentially expressed proteins. Vertical line over 0 indicates value for condition control (+serum). Red bars absence of serum (-serum). Blue bars absence of serum supplemented with 10μM of DETA/NO (-serum + DETA/NO). Statistical significance Student´s test *p-value* < *0.005*. (**B**) Top biological functions displayed by significance score (-log(p-value)). *p-value* < *0.005*. (**C**) Pie chart for sub-cellular localization distributed by percentage of proteins with respect to the total of correctly identified proteins. (**D**) Pie chart for protein functions distributed by percentage of proteins with respect to the total of correctly identified proteins. DRR: DNA replication recombination repair.

extracellular regions (4%) (**Fig. 4C**). Annotated protein functions were as follows: 20% metabolic, 16% structural, 16% oxidoreductases, 12% chaperones of metabolism, 8% chaperones related with proteasome, 8% gene expression and 5 fractions of 4% for proteins of: ion transport, secretory proteins, RNA processing, proteins of the electron transporting chain and DNA binding proteins respectively (**Fig. 4D**). When mouse islets were studied under similar conditions, 13 proteins were identified. ATP5A1, HSPA8, KRT10, ENO1 and P4HB were also present in human islets. High variability in protein abundance of replicates did not allow us to perform quantitative analysis in this islet tissue (**Table S1** and **Fig. S1**).

Comparative analysis of proteomic profile of RINm5F cells and Human Islets

Comparative analysis of proteins differentially expressed by NO, reveals proteins exclusively present in RINm5F cells such as metabolic proteins HMGCS1, ADK, GAPDH and MDH1, mitochondrial proteins UQCRC2, VDAC1, ATP5A1, ATP5C1, proteins involved in protein metabolism PSMD13, PSMA7, EEF1A1, RPSA, ERLIN2; antioxidants proteins PRDX1, GSTM1, structural proteins KRT8, ACTL6A, TUBA1C, CFL1, and the chaperone HSP90AB1. On the other hand, HPI expresses specifically chaperones HSPA5, HSPA9, HSP90AA1, protein disulphide isomerases PDIA6 and P4HB, structural proteins KRT1, KRT10, ACTG1, TUBA1B and TUBB, metabolic proteins GANAB, ALDH1, ALDH1A1, ENO1 and TPI1 and a protein involved in secretory machinery SCGN (Secretagogin). Finally, 3 proteins are found differentially expressed in both proteomes (HSPA8, PRDX2, ATP5A1) (**Table 1 and 2**). Based on these data, protein interaction networks were generated using Ingenuity Pathway Analysis (IPA) to visualize the effect of the treatment with NO on the proteome of cells grown in the absence of serum (**Figs. 5 and 6**). This approach allows to identify putative mechanisms shared in both species. From all the differentially expressed proteins, 79.3% (23/29) of the identified proteins in RINm5F cells (**Fig. 5A and B**) and 68% (17/25) in HPI (**Fig. 6A and B**) were mapped in independent networks. In RINm5F cells, p38 MAPK, Akt, Ck2, p85(pik3r) CD3, NFκB, cytochrome C and actin were identified as hub molecules. Interestingly, it was found that NO regulates the expression of diverse components of 3 common signaling pathways in both cell types: Glucocorticoid receptor signaling (9 proteins), NRF2-mediated oxidative stress response (7 proteins) and eNOS signaling (6 proteins). A group of targets corresponding to mitochondrial dysfunction (4 proteins) was found only in RINm5F cells (**Fig. 5**). These pathways interact through common molecules such as: Akt, p85(pik3r) and Hsp90 family. These data suggest that NO controls the oxidative stress response in this insulin producing cell line through the regulation of heat shock proteins and acts in coordination with Akt/pi3K/MAPK/ NFκB signaling pathways. It is relevant to note that in the absence of serum there is a regulation of some proteins of the mitochondrial respiratory chain. For instance, a decrease of ATP5C1 and UQCRC2 as well as an increase of ATP5A1 was found. These proteins have a completely opposed expression pattern (**Fig. 5A and B**) in NO-treated cells. Additionally, culture under serum deprivation conditions promotes the expression of proteins that participate in oxidative stress (PRDX1, TUBA1C, PSMD13, PSMA7, NME2, and HSP90AB1), and again NO has an opposite effect on their expression. (**Fig. 5B**).

With regard to the protein profile in HPI, the analysis reveals that insulin, Akt, NFκB, Ikbb, Erk1/2, p85(pik3r) and Pkc were found as hubs, despite the fact that their expression level is not affected by the experimental manipulations tested. (**Fig. 6A and B**). Additionally, heat shock family proteins (HSPA5, HSPA9, HSP90AA1, HSPA8) were found to mediate interaction between eNOS signaling and glucocorticoid receptor and furthermost with NRF2-mediated response. These pathways converge in 4 molecules: Akt, p85(pik3r), HSP90 and the ATPase complex. A possible regulation of the cytoplasm organization is evidenced by the regulation of ACTG1 by NRF2-mediated oxidative stress response, and interacting with TUBA1B, TUBB, KRT10. Other proteins associated with the network and also involved in response to oxidative stress include VCP related with the activity of 14-3-3 epsilon (YWHAE) (**Fig. 6B**).

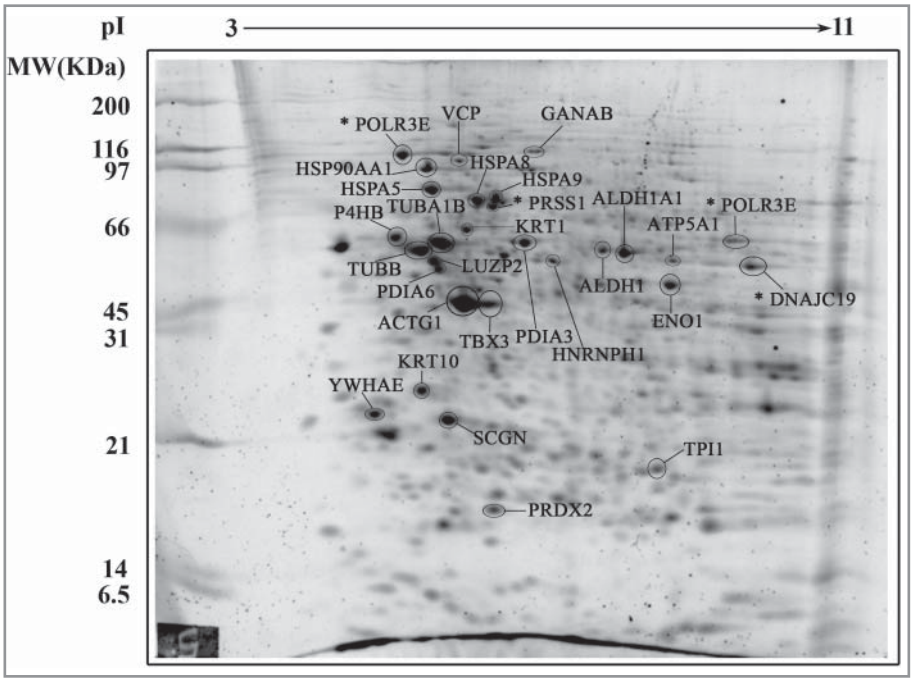

Figure 3. Representative 2-D gel map of human pancreatic islets. Protein extracts were loaded onto an IPG strip (pH 3 – 11) and subsequently separated by molecular weight in a 12% SDS-PAGE. Fluorescent staining was performed by directly incubating gels in SYPRO Ruby Protein Gel stain overnight. The spots were analyzed by MS-MALDI-TOF/TOF. Spots for differentially expressed proteins are indicated. * Indicates proteins with a Mascot Protein Score for identity less than 71.

Discussion

There is considerable evidence on the protective role of NO in a number of cell types including human and murine pancreatic β cells.[10,12-18] The mechanisms involved in the process remain, however, to be fully substantiated. Proteome analysis provides an informative approach to the issue. In the present study, we have analyzed the proteomic profile of rodent and human insulin producing cells in order to understand global changes that occur following exposure to protective levels of NO. Previous reports in the literature have depicted the protein profile of pancreatic islet tissue challenged with deleterious conditions such as exposure to inflammatory cytokines or high NO.[1,2,4,5,19-22] The present study provides evidence on the protein landscape underlying the survival response of pancreatic β cells to stressful conditions. The response of β cell to serum deprivation involves organelles such as mitochondria (ROS/RNS response) and ER (unfolding protein response). We have observed in this study that NO treatment contributes to the regulation of proteins related with these organelles in a protective response against oxidative stress; among these, chaperons of HSP family play an instrumental role by stabilizing partially unfolded proteins. In this respect, biological functions such as Small molecule biochemistry and Cell death and Survival stand out in RINm5F cells, while Post-translational modification and Protein folding are relevant in HPI (**Figs. 2B and 4B**). In addition analysis of the sub-cellular distribution shows that mitochondrial response prevails in RINm5F cells and while ER response is more apparent in HPI (**Figs. 2C and 4C**).

It is known that serum deprivation (SD) induces stress and affects cell survival in β cells.[23] Additionally, in other cellular models the consequence of SD is an increase in the production of ROS that could lead mitochondrial dysfunction and apoptosis.[24] Thus, in RINm5F cells, serum deprivation induced an increase of PRDX1 and HSP90AB1, while the expression of PRDX2 and HSPA8 decreased. NO restored the expression levels of these proteins, close to levels in cells cultured in the presence of serum (**Figs. 2A and 5**). With the exception of HSPA5, expression of heat shock proteins in HPI was also regulated by these experimental manipulations. Thus, expression levels of PRDX2, P4HB and PDIA6 were increased when cells were cultured without serum and NO treatment restored protein levels to control (+ serum) conditions. The expression of chaperones of HSP family such as HSP90AA1 and HSPA8 as well as the recovery of HSPA5 expression indicates a role for ER in the activation of the unfolded protein and oxidative stress responses.[9,25] Additionally, PRDX2 plays a protective role on oxidative stress induced apoptosis.[26] Little is known, however, about the cellular distribution and function of PRDX2 in human pancreatic islet cells. Increased levels of PRDX2 protein are found in serum-deprived HPI and NO treatment decreased the expression to values below the control condition (+ serum). This could be part of the protective response together with proteins such as protein disulfide isomerases (PDIA6, P4HB). As for RINm5F cells, PRDX1 could take over the oxido-reductive function. PRDX2 by contrast diminishes in the absence of serum and NO increases the expression to values above the control condition (+ serum).

Table 2. Identification of proteins differentially expressed after treatment with 10μM of DETA/NO in absence of serum in Human Pancreatic Islets

Spot ID	Official symbol	Name	Protein MW/PtdIns	No. peptides identified MASCOT	Mascot Protein Score	Biological Process
1	POLR3E	Polymerase (RNA) III (DNA directed) polypeptide E (80kD)	99101.4 /9.47	11	50 *	Cell Death and Survival
2	GANAB	Glucosidase, α; neutral AB	107262.8/ 5.74	28	578	Metabolism
3	VCP	Vasolin containing protein	84954.4 /5.16	32	390	Cell Death and Survival
4	HSP90AA1	Heat shock protein 90kDa α (cytosolic), class A member 1	80579.1/ 5.26	26	800	Cell Death and Survival
5	HSPA5	Heat shock 70kDa protein 5 (glucose-regulated protein, 78kDa)	68354.4 /5.15	31	1060	[a]Cell Death and Survival
6	HSPA9	Heat shock 70kDa protein 9 (mortalin)	73929.9 /5.81	18	582	[a]Cell Death and Survival
7	HSPA8	Heat shock 70kDa protein 8	70989.2 /5.24	22	837	Cell Death and Survival
8	PRSS1	Protease, serine, 1 (trypsin 1)	9219 /10.01	3	37 *	Metabolism
9	KRT1	Keratin 1	66149/ 8.16	13	76	Cell Proliferation
10	P4HB	Prolyl 4-hydroxylase, β polypeptide	57453.7 /4.73	28	875	Cell Proliferation
11	TUBA1B	Tubulin α-1B	46781/ 4.96	19	648	Cell Proliferation
12	PDIA3	Protein disulfide isomerase family A, member 3	54541.4 /5.61	22	407	Cell Death and Survival
13	POLR3E	Polymerase (RNA) III (DNA directed) polypeptide E (80kD)	99101.4 /9.47	10	48 *	Cell Death and Survival
14	TUBB	Tubulin, β class I	48319.4 /5.17	26	772	Cell Proliferation
15	ALDH1A1	Aldehyde dehydrogenase 1	51742.4 /6.68	17	671	Metabolism
16	LUZP2	Leucine zipper protein 2	10021.2 /7.94	8	75	Development
17	ALDH1A1	Aldehyde dehydrogenase 1 family, member A1	51742.4 /6.68	17	728	Metabolism
18	HNRNPH1	Heterogeneous nuclear ribonucleoprotein H1 (H)	43790.1 /6.29	7	98	Cell Death and Survival
19	ATP5A1	ATP synthase, H^+ transporting, mitochondrial F1 complex, α subunit 1, cardiac muscle	59827.6 /9.16	27	735	Cell Death and Survival
20	PDIA6	Protein disulfide isomerase family A, member 6	46512.3 /4.95	14	907	[a]Cell Death and Survival
21	DNAJC19	DnaJ (Hsp40) homolog, subfamily C, member 19	17412,9/9,71	6	38 *	Cell Death and Survival
22	ENO1	Enolase 1, (α)	42720.9 /6.97	25	673	Metabolism
23	TBX3	T-box 3	57754.1 /6.95	9	84	Development
24	ACTG1	Actin, gamma 1	41334.6 /5.56	15	636	Cell Proliferation
25	KRT10	Keratin 10	56862.9/ 5.05	11	81	Cell Death and Survival
26	YWHAE	Tyrosine 3-monooxygenase/ tryptophan 5-monooxygenase activation protein, epsilon	26911.5 /4.92	16	431	Cell Death and Survival
27	SCGN	Secretagogin, EF-hand calcium binding protein	32190.2 /5.25	23	603	Cell Proliferation
28	TPI1	Triosephosphate isomerase 1	26937.8 /6.45	20	774	Metabolism
29	PRDX2	Peroxiredoxin 2	16165.3 /5.71	8	343	[a]Cell Death and Survival

*Protein score is −10*Log(P), where P is the probability that the observed match is a random event. Protein scores greater than 71 are significant ($P < 0.05$).
[a]Involved in β-cell survival

Additional proteins involved in the oxidative stress response and in the cell survival triggered by NO are mitochondrial ATPase F0/F1 subunits (ATP5A1 in HPI, ATP5A1 and ATP5C1 in RINm5F cells). In addition to their role in oxidative metabolism, these proteins are involved in the anti-apoptotic response in different cell types.[27-29] Likewise, the unfolded protein response induced by NO could be also due to the regulation of protein disulfide isomerases (PDIA6 and P4HB (PDIA1) in HPI improving the protein folding including insulin for its accurate secretion.[30] Increments in ATP5A1, P4HB and HSPA8 and other proteins such as HSPD1, ATP6V1B1 and HSP90B1 were also detected in NO-treated, serum-deprived mouse pancreatic islets when compared with islets cultured under serum withdrawal, despite having used a different strategy for analyzing the spots (**Table S1** and **Figure S1**). It is also relevant to note the existence of species differences in keratin expression. Thus, KRT8 is expressed in RINm5F cells while KRT1 and KRT10 are expressed in HPI following NO treatment. These type II cytoskeletal proteins not only provide structural stability and protection from cell stress but they also have role in non-acute islet

stress response, as proposed recently.[31] Additionally, KRT proteins have been detected in 2-D protein analysis of glucose-responding mouse islets, INS-1E cells, and human islets.[6] Our study also shows that proteins involved in the impairment of glucose-induced insulin release such as TUBB5, KRT8, PEBP1 and PDIA3 (RINm5F cells), HSPA5, ENO1, P4HB, SCGN, PRDX2 and PDIA6 (HPI) and HSP90B1 (Endoplasmin), ENO1, ATP6V1B1 (mouse islets) are regulated by NO.[32,33] Overall, these results provide evidence that NO induces changes in the expression of a group of proteins involved in the β cell secretory response.

Serum deprivation activates stress and cell death signals in pancreatic β cells.[23] This condition has been shown to increase intracellular ROS levels in other cell types.[34] Our group has shown previously that generation of low amounts of NO protects efficiently against this type of cell death.[10,12] Specifically, dysfunction of unfolded protein response during endoplasmic reticulum stress plays a role in impairment of pancreatic β cell function in both Type 1 and type 2 diabetes.[35,36] Our study reports that serum withdrawal downregulates a set of proteins involved in survival (HSPA5, PDIA6, PRDX1, PRDX2) and homeostasis (TUBB5 or ACTG1) of pancreatic β cells In this regard, HSPA5 (Grp78) plays a relevant role in protection against ER stress or cytokine-induced β cell death.[37-39] Recovery of expression levels following NO treatment supports a role for this protein in the cell response to stressful conditions. IPA analysis provides a wider view of the NO actions in this model of cell damage. In addition, 23 out of 29 identified proteins map in a network formed by 4 significant signaling pathways: Glucocorticoid Receptor signaling, eNOS signaling NRF2-mediated Oxidative Stress Response and Mitochondrial Dysfunction in RINm5F cells (**Figs. 5** and **6**). As for HPI, 17 out of 25 identified proteins were mapped in a network resembling that of insulinoma cells, with the exception of mitochondrial dysfunction. It is entirely possible that endoplasmic reticulum is involved on the activated survival response in HPI because of the higher number of ER proteins (20%) with respect to mitochondrial proteins (8%) (**Fig. 4C**), while the opposite takes place in RINm5F cells in which fewer ER proteins (7%) were found with respect to mitochondrial proteins (14%) (**Fig. 2C**). The networks generated for both cell types corroborate that NO signaling is being regulated by the treatment and share components with the glucocorticoid response and NRF2-mediated oxidative stress response in close association with chaperones and protein disulphide isomerases also reported in this study. The former has been implicated in β cell dysfunction through the activation of the unfolded protein response following endoplasmic reticulum stress.[40] The finding that NO shares with glucocorticoids the regulation of some HSPs and PI3K/Akt pathway opens the possibility to study whether low NO blocks the β cell damage produced by these anti-inflammatory drugs. With regard to NRF2 (NF-E2-related-factor-2), it has been postulated that regulates the expression of antioxidant-enzyme genes and that it might play a role in pancreatic β cell defense against RNOS.[41] Therefore, the interaction of proteins shown in the pathways identified in our study show that low concentrations of NO protects β cells from the effects of serum deprivation which may lead to apoptotic cell death or impair homeostatic functions.

Based on these observations we conclude that low concentrations of NO elicit a protective response in murine and human pancreatic islets cells exposed to serum deprivation which involves the expression of proteins related to mitochondrial function in murine pancreatic β cells and to ER function in HPI.

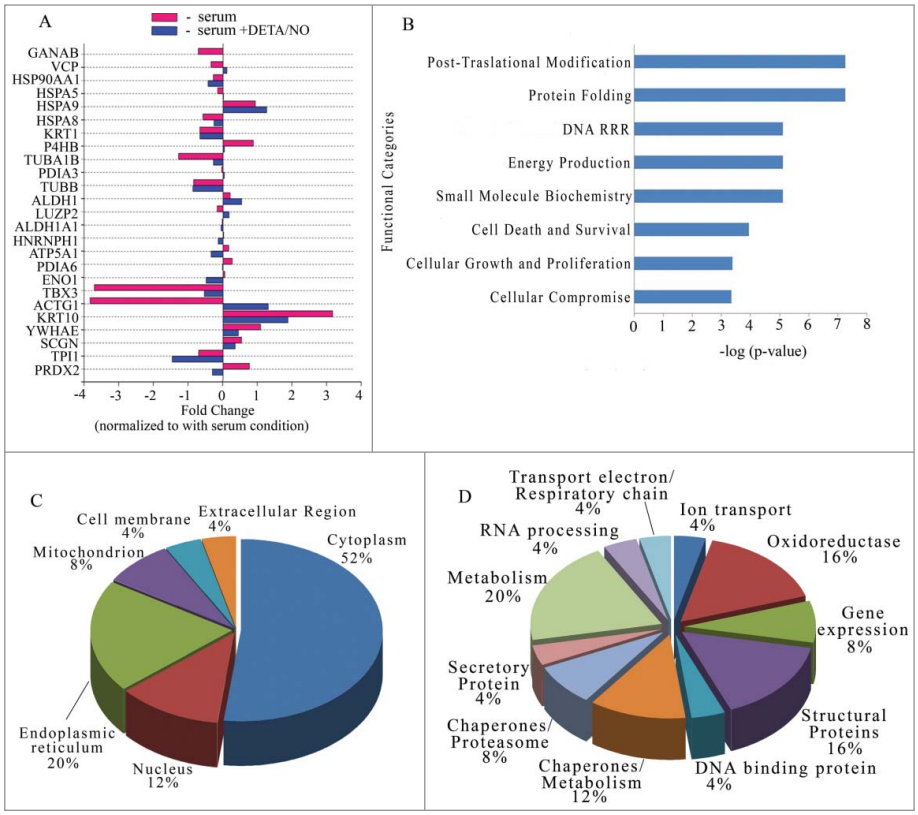

Figure 4. Characterization of differentially expressed proteins in human pancreatic islets. (**A**) Bar graph of the fold changes for differentially expressed proteins. Vertical line over 0 indicates value for condition control (+serum). Red bars absence of serum (-serum). Blue bars absence of serum supplemented with 10μM of DETA/NO (-serum + DETA/NO). Statistical significance Student´s test *p-value* < *0.005* (**B**) Top biological functions displayed by significance score (-log(p-value)). *p-value* < *0.005*. (**C**) Pye chart for sub-cellular localization distributed by percentage of proteins with respect to the total of correctly identified proteins. (**D**) Pie chart for protein functions distributed by percentage of proteins with respect to the total of correctly identified proteins. DRR: DNA replication recombination repair.

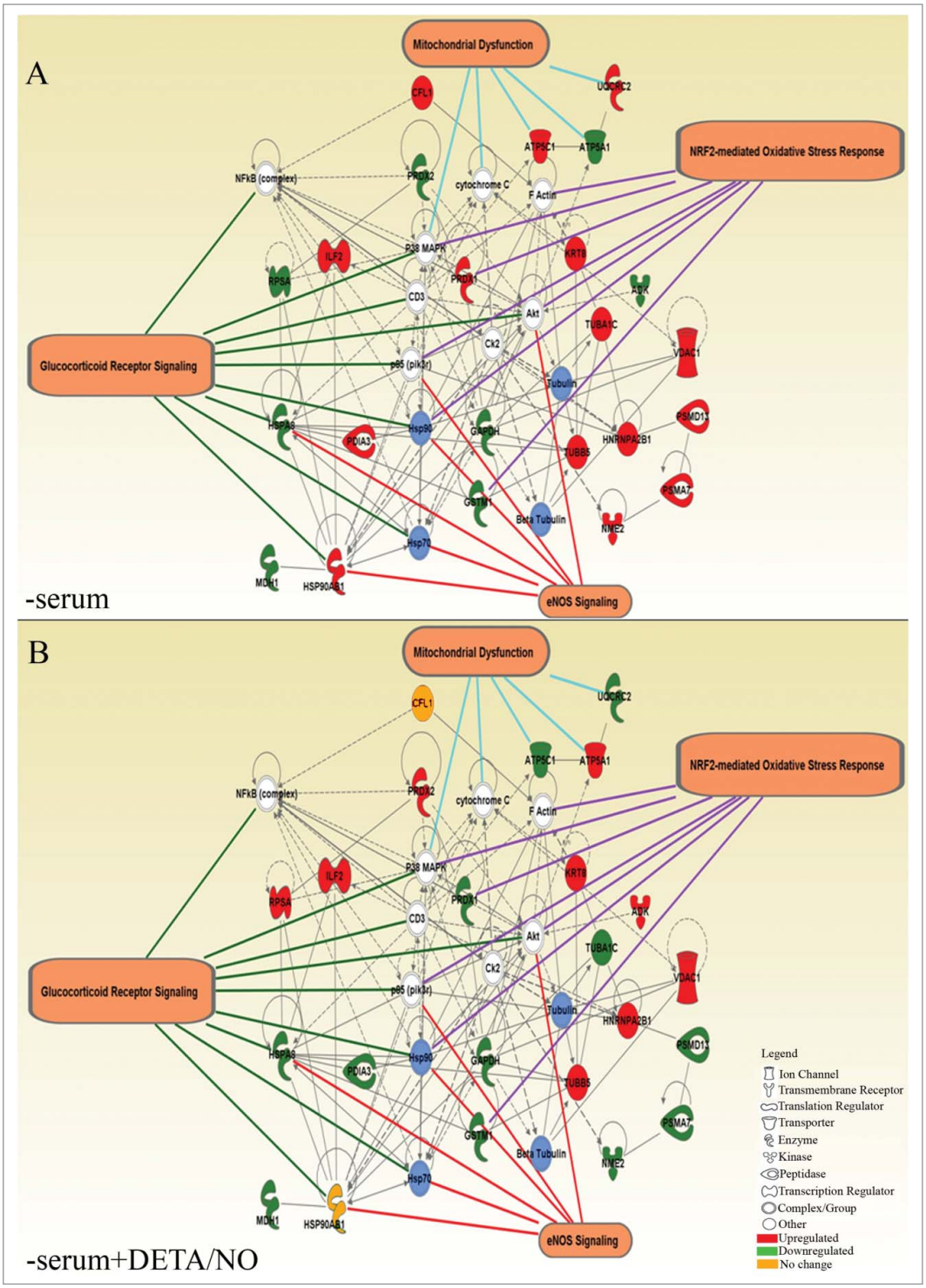

Figure 5. Interaction networks generated from a set of differentially expressed proteins detected in RINm5F cells. (**A**) Cultured in absence of serum (-serum) and (**B**) cultured in absence of serum supplemented with 10μM of DETA/NO. Proteins with red background are upregulated, green = downregulated, orange = no change. Blue shading denotes groups or complexes of proteins regulated with the treatment. White shading indicates proteins interacting in the network but not regulated by the treatment. The more representative networks are shown with the respective targets.

Whether the species differences reported here applies to other models of β cell stress remains to be established.

Materials and Methods

Cell culture conditions

RINm5F rat insulinoma cells were cultured for 24 hours in 175cm^2 culture flasks (Greiner Bio-One, North America) in a 10000 cells/cm^2 ratio and maintained in RPMI 1640 (Lonza, Switzerland) supplemented with 100μg/ml streptomycin (Gibco Bethesda MD USA), 100U/ml penicillin (Gibco), 2.5μg/mL amphotericin B (Gibco), 2mM glutamine (Gibco), and 10% fetal bovine serum (FBS) (Gibco), in a humidified atmosphere of 5% CO_2 at 37°C. Cells used for experiments were from passages 20-24. Pancreatic islets were obtained in collaboration with the European Consortium for Islet Transplantation (ECIT Switzerland) from a human cadaveric donor without primary or secondary pancreatic pathology. Islets were isolated using the Ricordi method.[42] Isolated islets were pooled, washed once in PBS 1X and seeded in 6 well cell culture plates (Greiner Bio-One, North America) at density of 1000 islets per well. The islets were incubated in suspension for 1-3 days at 37°C and 5% CO_2 in CMRL medium (CMRL 1066 w/o phenol red from School of Medicine Diabetes Research Institute University of Miami, cat. N° 99-663-CV) supplemented with 10% fetal bovine serum (Sigma, Missouri, USA), 100U/ml penicillin (Gibco), 100μg/ml streptomycin (Gibco), 2mM glutamine (Gibco) and 0.01mg/mL gentamicin (Sigma). The

experimental procedure with human material was approved by the Research Ethics Authority of University Pablo de Olavide. For mouse studies, 400 – 600 pancreatic islets isolated by collagenase digestion were used per condition corresponding to approximately 50 μg of protein. Isolated islets were incubated for 3 days at 37°C and 5% CO_2 in RPMI 1640 medium containing 11mM glucose and supplemented with 10% FBS, 2mM glutamine (Gibco), 100U/ml penicillin and, 100μg/ml streptomycin. For treatments, RINm5F cells, mouse and human islets were cultured in either FBS-free medium or in FBS-free medium supplemented with 10μM of the NO donor (diethylenetriamine/NO adduct - DETA-NO (Sigma) for 19h. After treatments, cells were stored at −80°C until 2-D-PAGE analysis.

Sample preparation for 2-D SDS-PAGE

For RINm5F, 3×10^6 cells from 3 different passages were cultured under 3 experimental conditions. For HPI, 180- 200 islets were cultured in triplicate. For mouse pancreatic islets, batches of 100-200 islets from 15 mice were cultured in triplicate. At the end of the culture period islets and trypsinized RINm5F cells were collected by sedimentation and centrifugation respectively and stored at −20°C. For protein separation, samples were pooled in a single tube per condition. Cell pellets were washed in phosphate-buffered saline and resuspended in 100 μl of lysis buffer (7M urea, 2M thiourea, 3% (w/v) CHAPS, 40mM Tris base, 1% (w/v) DTT, and a mixture of protease inhibitors (SigmaFast, Sigma Aldrich). Samples were disrupted by sonication on ice at 30 kV for 5 minutes (Ultrasonic, Raypa) and then

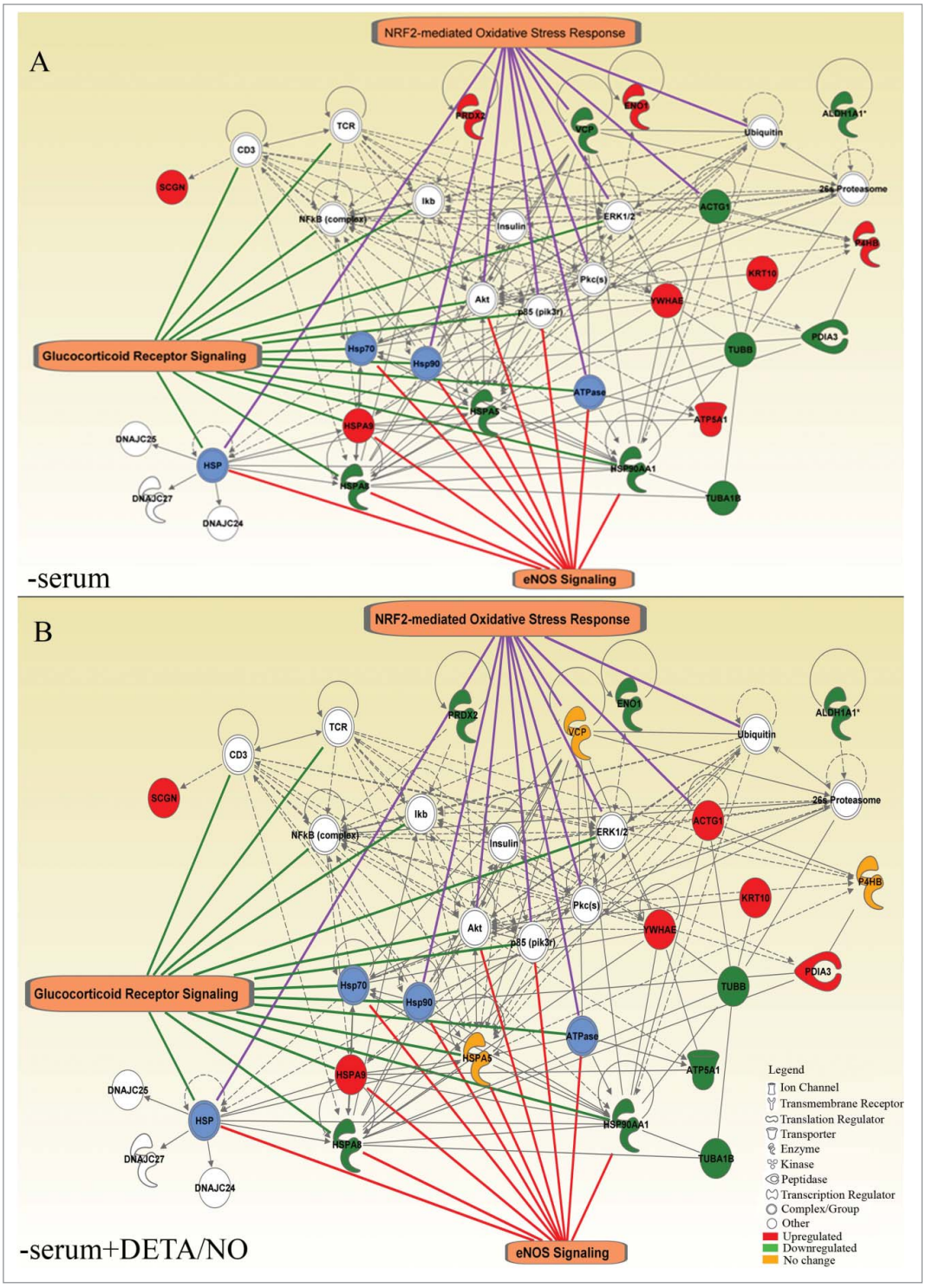

Figure 6. Interaction networks generated from a set of differentially expressed proteins detected in human pancreatic islets. (**A**) Cultured in the absence of serum (- serum) and (**B**) Cultured in absence of serum supplemented with 10μM of DETA/NO (-serum + DETA/NO). Blue shading denotes groups or complexes of proteins regulated with the treatment. White shading corresponds to proteins of the network not regulated by the treatment. The more representative networks are shown with the respective targets.

centrifuged for 13 min at 16,000 × g (4°C) to precipitate all non-soluble proteins and membrane fractions. Supernatants were then transferred to a new tube. Samples were desalted with one volume of 10 % aqueous TCA for 1 hour at −20°C. After this, samples were centrifuged at 16,000 × g at 4°C for 15 minutes and washed 3 times with ice cold acetone and air dried for 5 minutes. Samples were then resuspended in 200 μl rehydration buffer (7M urea, 2M thiourea, 3% (w/v) CHAPS, 1% (w/v) DTT). In the case of human islets, cells were lysed in 7M urea, 2 M thiourea, 4%CHAPS with 30mM DTT. Proteins were then precipitated with *chloroform-methanol* solution and dissolved in 7M Urea, 2M thiourea and 4% CHAPS. A second precipitation was carried out by using 2-D Clean-up kit (GE Healthcare) and dissolved in 7M urea, 2M thiourea and 4% CHAPS.

2-D SDS-PAGE

2-D electrophoresis were carried out at the proteomic facility in CABIMER, 3 gels for RINm5F and HPI and 2 gels for mouse pancreatic islets by experimental condition. 100 μg of RINm5F cell protein, was applied by passive rehydration to pre-cast immobilized pH gradient strips (24cm; pH 3–10 NL GE Healthcare) for 6 hours in 300 μl of a solution containing 7M Urea, 2M Thiourea, 3% CHAPS, 50mM DTT, 0.8% IPG buffer and bromophenol blue. Pooled samples were separated according to their isoelectric point in an Ettan IPGphor II system (GE, Amersham Biosciences). The complete process was tracked with the Ettan IPGphor control software (version 1.01.03) (GE Healthcare). The first dimension was ended when the current reached a stable phase (at ≈68 kV-h).

Prior to the second dimension, the strips were equilibrated during 2 intervals of 15 min each in an equilibration buffer (7M urea, 2M Thiourea, 30% (v/v) glycerol, 2% (w/v) SDS, bromophenol blue, and 50mM Tris-HCl, (pH 8.8) containing 1% (w/v) DTT in the first step and 4% (w/v) iodoacetamide in the second step. Equilibrated strips were placed on top of 10% SDS-polyacrylamide gel and separated on an Ettan DaltSix system (GE Healthcare) until the bromophenol blue front left the gel and was no longer visible. After second dimension the gels were stained with silver nitrate according to.[43] This protocol is compatible with mass spectrometry downstream analysis. For human islet material, the proteomic 2-D gel analysis and mass spectrometry was carried out at the University of Cordoba proteomics facility (UCO SCAI), a member of Carlos III Network Proteomics Platform (ProteoRed-ISCIII). Briefly, pre-cast immobilized pH gradient strips (7cm; pH 3–11 NL GE Healthcare) were used. The strips were equilibrated with a solution containing 6M urea, 20% glycerol, 2% SDS, 375mM Tris (pH 8.8) reduced with 2% DTT and 2,5% iodoacetamide for the first-dimensional separation and run for a total focusing time of 18 kV/h directly applied to a 12% SDS-PAGE gel for electrophoresis overnight at 60-mA constant for the second-dimensional separation.

Then, 2-D gels were pre-incubated in a fixative solution of 7% acetic acid and 10% methanol for 30 min Fluorescent staining of 2-D gels was performed by directly incubating gels in SYPRO Ruby Protein Gel stain overnight. After staining, gels were incubated in the fixation solution for 30 min to wash residual dye to obtain even lower residual matrix background staining. The SYPRO Ruby-stained image was scanned at an excitation wavelength of 400 nm and an emission wavelength of 535nm. All the images were collected on a Molecular Imager FX ProPlus (BioRad).

Image Analysis

Analysis of the raw scans was performed using PD Quest 7.4 (BioRad) software available from Supercomputing and Bioinnovation Center at University of Málaga (SCBI-UMA). The software allows automatic, accurate detection and quantification of protein spots by calculation of the spot volumes thus setting the accurate range of spots by indication of the faintest and the most intense spots. Firstly, the generation of the master gel was performed by a hierarchic analytical procedure, where the analysis of the 3 gel replicates from each experimental condition result in a representative composite that will hold information of all spots identified in the triplicates. The corresponding reference images were analyzed in a reference matched image. Then, the spots center was detected using Laplacian algorithm. The sum of the pixel intensity values within the perimeter (volume) was calculated and a value of integrated intensity was obtained. The pixel volume of each spot was calculated based on the intensity and area of the spots, followed by the normalization with respect to the total pixel volume of all the spots in the gel image in the control condition (+serum). The pixel volume of each spot was the base to compare protein expression between the control condition (+serum) and the experimental conditions. A statistical approach was applied when determining differentially expressed proteins using the PDQuest software. Student's t-test was performed with 95% significance level to determine which proteins were differentially expressed between control (+serum) and experimental conditions. Image analysis of 2-D gels from mouse islets was carried out by visual selection of the spots displaying size change in the different experimental conditions. The selected spots were analyzed by mass spectrometry at the UCO-SCAI proteomics facility

Mass Spectrometry

Spots were excised automatically in a ProPic Station (Genomic Solutions). The gel pieces were washed with 100 mM NH_4HCO_3, dehydrated with acetonitrile, and then dried completely in the vacuum concentrator. For sequence-specific digestion the gel pieces were re-swollen in minimal volumes of 25 mM NH_4HCO_3 containing 12.5 ng/μl trypsin and incubated at 37°C for 12 hours. The peptide extracts were purified on reversed-phased C18 ZipTip pipette tips (Millipore Corp.), and eluted with a solvent containing *cyano-4*-hydroxycinnamic *acid* matrix (3 mg/ml in 70% acetonitrile, 0.1% trifluoroacetic acid). MALDI-TOF-mass spectrometry and tandem TOF/TOF mass spectrometry of the peptides was performed on a 4800 Proteomics Analyzer (Applied Biosystems). Peptide mass maps were acquired in reflectron mode (20 keV accelerating voltage). Trypsin autolytic

peptides (m/z = 842.51, 1045.56, and 2211.10) were used to internally calibrate each spectrum to a mass accuracy within 20 ppm. When trypsin autolytic peptides were not detected (in the case of very abundant proteins), an external standard was applied on the target from a neighboring sample (obtaining a mass accuracy within 50 ppm). Individual ions from each spectrum were inspected for resolution and isotopic distribution to identify potentially different peptides of similar mass (with overlapping isotopic distributions) and to rule out low-resolution ions that may result from metastable decomposition. Protein identifications from MALDI-TOF peptide mass maps are based on the masses of the tryptic peptides. Tandem mass spectrometry (MALDI-TOF/TOF) was used to generate limited amino acid sequence information on selected ions if additional confirmation was required. Searches were performed without constraining protein molecular weight or isoelectric point, and allowed for carbamidomethylation of cysteine, partial oxidation of methionine residues, and one missed trypsin cleavage. Highest confidence identifications have statistically significant search score(s), and are consistent with the gel region from which the protein was excised (MW and pI), and account for the majority of the ions present in the mass spectrum. Ions specific for each sample (discrete from background and trypsin-derived ions) were then used to interrogate human sequences entered in the SWISS-PROT and NCBInr databases using the MASCOT (www.matrixscience.com) database search algorithms.

Network Analysis

Association of the identified proteins with canonical pathways was performed using the Ingenuity Pathways Analysis (IPA) tool (www.ingenuity.com). A dataset containing genes´ official symbols for each correctly identified protein, obtained from Gene Database (http://www.ncbi.nlm.nih.gov/entrez/query.fcgi?db=gene), was uploaded in the IPA suite. IPA access was obtained from SCBI-UMA. Each ID was mapped to its corresponding gene object in the Ingenuity Pathways Knowledge Base. These genes, called Focus Genes, were overlaid onto a global molecular network (graphical representation of the molecular relationships between genes/gene products) developed from information contained in the Ingenuity Pathways Knowledge Base. Networks of these Focus Genes were then algorithmically generated based on their connectivity. The network genes associated with biological functions in the Ingenuity Pathways Knowledge Base were considered for the analysis. Fischer's exact test was used to calculate a p-value determining the probability that each biological function assigned to that network is due to chance alone. The significance of the association between the data set and the canonical pathway was measured in 2 ways: A ratio of the number of genes from the data set that map to the pathway divided by the total number of genes that map to the canonical pathway is displayed, and Fischer's exact test was used to calculate a p value determining the probability that the association between the genes in the data set and the canonical pathway is explained by chance alone represented as –log(*p-value*).

Disclosure of Potential Conflicts of Interest

No potential conflicts of interest were disclosed

Funding

This study was supported by grants from Consejería de Igualdad, Salud y Políticas Sociales. Junta de Andalucía (PI105/2010) and Consejería de Economía, Innovación, Ciencia y Empleo. Junta de Andalucía (CTS- 7127/2011) to FJ Bedoya; from Consejería de Igualdad, Salud y Políticas Sociales. Junta de Andalucía, ISCIII co-funded by Fondos FEDER (RED TERCEL - RD06/0010/0025; RD12/0019/0028 and PI10/00964, Consejería de Economía, Innovación, Ciencia y Empleo (P10.CTS.6505) and the Ministerio de Salud y Políticas Sociales (Programa de Terapias Avanzadas, TRA-120) to B Soria; from Consejería de Igualdad, Salud y Políticas Sociales (PI0022/2008) and from Consejería de Economía, Innovación, Ciencia y Empleo. Junta de Andalucía (PAI, BIO311) to F Martín and from Servicio Andaluz de Salud (SAS 11245) and Ministerio de Economía y Competitividad-Secretaría de Estado de Investigación Desarrollo e Innovación (IPT-2011-1615-900000) to JR Tejedo.

Supplemental Material

Supplemental data for this article can be accessed on the publisher's website.

References

1. John NE, Andersen HU, Fey SJ, Larsen PM, Roepstorff P, Larsen MR, Pociot F, Karlsen AE, Nerup J, Green IC, et al. Cytokine- or chemically derived nitric oxide alters the expression of proteins detected by two-dimensional gel electrophoresis in neonatal rat islets of Langerhans. Diabetes 2000; 49:1819-29; PMID:11078448; http://dx.doi.org/10.2337/diabetes.49.11.1819
2. Larsen PM, Fey SJ, Larsen MR, Nawrocki A, Andersen HU, Kahler H, Heilmann C, Voss MC, Roepstorff P, Pociot F, et al. Proteome analysis of interleukin-1beta–induced changes in protein expression in rat islets of Langerhans. Diabetes 2001; 50:1056-63; PMID:11334408; http://dx.doi.org/10.2337/diabetes.50.5.1056
3. Ahmed M, Forsberg J, Bergsten P. Protein profiling of human pancreatic islets by two-dimensional gel electrophoresis and mass spectrometry. J Proteome Res 2005; 4:931-40; PMID:15952740; http://dx.doi.org/10.1021/pr050024a
4. Fernandez C, Fransson U, Hallgard E, Spegel P, Holm C, Krogh M, Warell K, James P, Mulder H. Metabolomic and proteomic analysis of a clonal insulin-producing beta-cell line (INS-1 832/13). J Proteome Res 2008; 7:400-11; PMID:18062666; http://dx.doi.org/10.1021/pr070547d
5. Bergsten P. Islet protein profiling. Diabetes, Obes Metab 2009; 11 Suppl 4:97-117; PMID:19817793; http://dx.doi.org/10.1111/j.1463-1326.2009.01111.x
6. Ahmed M. Proteomics and islet research. Adv Exp Med Biol 2010; 654:363-90; PMID:20217506; http://dx.doi.org/10.1007/978-90-481-3271-3_16
7. Kurohane Kaneko Y, Ishikawa T. Dual role of nitric oxide in pancreatic beta-cells. J Pharmacol Sci 2013; 123:295-300; PMID:24285083; http://dx.doi.org/10.1254/jphs.13R10CP
8. Tsuura Y, Ishida H, Hayashi S, Sakamoto K, Horie M, Seino Y. Nitric oxide opens ATP-sensitive K+ channels through suppression of phosphofructokinase activity and inhibits glucose-induced insulin release in pancreatic beta cells. J Gen Physiol 1994; 104:1079-98; PMID:7699364; http://dx.doi.org/10.1085/jgp.104.6.1079
9. Oyadomari S, Takeda K, Takiguchi M, Gotoh T, Matsumoto M, Wada I, Akira S, Araki E, Mori M. Nitric oxide-induced apoptosis in pancreatic beta cells is mediated by the endoplasmic reticulum stress pathway. Proc Natl Acad Sci U S A 2001; 98:10845-50; PMID:11526215; http://dx.doi.org/10.1073/pnas.191207498
10. Tejedo JR, Cahuana GM, Ramirez R, Esbert M, Jimenez J, Sobrino F, Bedoya FJ. nitric oxide triggers the

phosphatidylinositol 3-kinase/Akt survival pathway in insulin-producing RINm5F cells by arousing Src to activate insulin receptor substrate-1. Endocrinology 2004; 145:2319-27; PMID:14764634; http://dx.doi.org/10.1210/en.2003-1489
11. Johnson JD, Bernal-Mizrachi E, Alejandro EU, Han Z, Kalynyak TB, Li H, Beith JL, Gross J, Warnock GL, Townsend RR, et al. Insulin protects islets from apoptosis via Pdx1 and specific changes in the human islet proteome. Proc Natl Acad Sci U S A 2006; 103:19575-80; PMID:17158802; http://dx.doi.org/10.1073/pnas.0604208103
12. Cahuana GM, Tejedo JR, Hmadcha A, Ramirez R, Cuesta AL, Soria B, Martin F, Bedoya FJ. Nitric oxide mediates the survival action of IGF-1 and insulin in pancreatic beta cells. Cell Signal 2008; 20:301-10; PMID:18023142; http://dx.doi.org/10.1016/j.cellsig.2007.10.001
13. Barsacchi R, Perrotta C, Bulotta S, Moncada S, Borgese N, Clementi E. Activation of endothelial nitric-oxide synthase by tumor necrosis factor-alpha: a novel pathway involving sequential activation of neutral sphingomyelinase, phosphatidylinositol-3' kinase, and Akt. Mol Pharmacol 2003; 63:886-95; PMID:12644590; http://dx.doi.org/10.1124/mol.63.4.886
14. Barsacchi R, Perrotta C, Sestili P, Cantoni O, Moncada S, Clementi E. Cyclic GMP-dependent inhibition of acid sphingomyelinase by nitric oxide: an early step in protection against apoptosis. Cell Death Differ 2002; 9:1248-55; PMID:12404124; http://dx.doi.org/10.1038/sj.cdd.4401095
15. Diet A, Abbas K, Bouton C, Guillon B, Tomasello F, Fourquet S, Toledano MB, Drapier JC. Regulation of peroxiredoxins by nitric oxide in immunostimulated macrophages. J Biol Chem 2007; 282:36199-205; PMID:17921138; http://dx.doi.org/10.1074/jbc.M706420200
16. Hess DT, Matsumoto A, Kim SO, Marshall HE, Stamler JS. Protein S-nitrosylation: purview and parameters. Nat Rev 2005; 6:150-66; PMID:15688001; http://dx.doi.org/10.1038/nrm1569
17. Kitiphongspattana K, Khan TA, Ishii-Schrade K, Roe MW, Philipson LH, Gaskins HR. Protective role for nitric oxide during the endoplasmic reticulum stress response in pancreatic beta-cells. Am J Physiol 2007; 292:E1543-54; PMID:17264231
18. Tejedo JR, Ramirez R, Cahuana GM, Rincon P, Sobrino F, Bedoya FJ. Evidence for involvement of c-Src in the anti-apoptotic action of nitric oxide in serum-deprived RINm5F cells. Cell Signal 2001; 13:809-17; PMID:11583916; http://dx.doi.org/10.1016/S0898-6568(01)00206-6
19. Cunningham JM, Green IC. Cytokines, nitric oxide and insulin secreting cells. Growth Regul 1994; 4:173-80; PMID:7756973
20. Kacheva S, Lenzen S, Gurgul-Convey E. Differential effects of proinflammatory cytokines on cell death and ER stress in insulin-secreting INS1E cells and the involvement of nitric oxide. Cytokine 2011; 55:195-201; PMID:21531147; http://dx.doi.org/10.1016/j.cyto.2011.04.002
21. Ortsater H, Bergsten P. Protein profiling of pancreatic islets. Expert Rev Proteomics 2006; 3:665-75; PMID:17181479; http://dx.doi.org/10.1586/14789450.3.6.665
22. Quintana-Lopez L, Blandino-Rosano M, Perez-Arana G, Cebada-Aleu A, Lechuga-Sancho A, Aguilar-Diosdado M, Segundo C. Nitric oxide is a mediator of antiproliferative effects induced by proinflammatory cytokines on pancreatic beta cells. Mediators Inflamm 2013; 2013:905175; PMID:23840099; http://dx.doi.org/10.1155/2013/905175
23. Ling Z, Hannaert JC, Pipeleers D. Effect of nutrients, hormones and serum on survival of rat islet beta cells in culture. Diabetologia 1994; 37:15-21; PMID:7512059; http://dx.doi.org/10.1007/BF00428772
24. Pandey S, Lopez C, Jammu A. Oxidative stress and activation of proteasome protease during serum deprivation-induced apoptosis in rat hepatoma cells; inhibition of cell death by melatonin. Apoptosis 2003; 8:497-508; PMID:14601556; http://dx.doi.org/10.1023/A:1025542424986
25. Gotoh T, Mori M. Arginase II downregulates nitric oxide (NO) production and prevents NO-mediated apoptosis in murine macrophage-derived RAW 264.7 cells. J Cell Biol 1999; 144:427-34; PMID:9971738; http://dx.doi.org/10.1083/jcb.144.3.427
26. Zhao F, Wang Q. The protective effect of peroxiredoxin II on oxidative stress induced apoptosis in pancreatic beta-cells. Cell Biosci 2012; 2:22; PMID:22709359; http://dx.doi.org/10.1186/2045-3701-2-22
27. Matsuyama S, Xu Q, Velours J, Reed JC. The Mitochondrial F0F1-ATPase proton pump is required for function of the proapoptotic protein Bax in yeast and mammalian cells. Mol Cell 1998; 1:327-36; PMID:9660917; http://dx.doi.org/10.1016/S1097-2765(00)80033-7
28. Vendemiale G, Grattagliano I, Caraceni P, Caraccio G, Domenicali M, Dall'Agata M, Trevisani F, Guerrieri F, Bernardi M, Altomare E. Mitochondrial oxidative injury and energy metabolism alteration in rat fatty liver: effect of the nutritional status. Hepatology 2001; 33:808-15; PMID:11283843; http://dx.doi.org/10.1053/jhep.2001.23060
29. Wang HQ, Xu YX, Zhao XY, Zhao H, Yan J, Sun XB, Guo JC, Zhu CQ. Overexpression of F(0)F(1)-ATP synthase alpha suppresses mutant huntingtin aggregation and toxicity in vitro. Biochem Biophy Res Comm 2009; 390:1294-8; PMID:19878659; http://dx.doi.org/10.1016/j.bbrc.2009.10.139
30. Rajpal G, Schuiki I, Liu M, Volchuk A, Arvan P. Action of protein disulfide isomerase on proinsulin exit from endoplasmic reticulum of pancreatic beta-cells. J Biol Chem 2012; 287:43-7; PMID:22105075; http://dx.doi.org/10.1074/jbc.C111.279927
31. Alam CM, Silvander JS, Daniel EN, Tao GZ, Kvarnstrom SM, Alam P, Omary MB, Hanninen A, Toivola DM. Keratin 8 modulates beta-cell stress responses and normoglycaemia. J Cell Sci 2013; 126:5635-44; PMID:24144696; http://dx.doi.org/10.1242/jcs.132795
32. Ahmed M, Bergsten P. Glucose-induced changes of multiple mouse islet proteins analysed by two-dimensional gel electrophoresis and mass spectrometry. Diabetologia 2005; 48:477-85; PMID:15729580; http://dx.doi.org/10.1007/s00125-004-1661-7
33. Dowling P, O'Driscoll L, O'Sullivan F, Dowd A, Henry M, Jeppesen PB, Meleady P, Clynes M. Proteomic screening of glucose-responsive and glucose non-responsive MIN-6 beta cells reveals differential expression of proteins involved in protein folding, secretion and oxidative stress. Proteomics 2006; 6:6578-87; PMID:17163442; http://dx.doi.org/10.1002/pmic.200600298
34. Andoh T, Chock PB, Chiueh CC. The roles of thioredoxin in protection against oxidative stress-induced apoptosis in SH-SY5Y cells. J Biol Chem 2002; 277:9655-60; PMID:11751890; http://dx.doi.org/10.1074/jbc.M110701200
35. Engin F, Yermalovich A, Nguyen T, Hummasti S, Fu W, Eizirik DL, Mathis D, Hotamisligil GS. Restoration of the unfolded protein response in pancreatic beta cells protects mice against type 1 diabetes. Sci Transl Med 2013; 5:211ra156; PMID:24225943; http://dx.doi.org/10.1126/scitranslmed.3006534
36. Engin F, Nguyen T, Yermalovich A, Hotamisligil GS. Aberrant islet unfolded protein response in type 2 diabetes. Sci Rep 2014; 4:4054; PMID:24514745; http://dx.doi.org/10.1038/srep04054
37. Wang M, Wang P, Peng JL, Wu S, Zhao XP, Li L, Shen GX. The altered expression of glucose-regulated proteins 78 in different phase of streptozotocin-affected pancreatic beta-cells. Cell Stress Chaperones 2009; 14:43-8; PMID:18597185; http://dx.doi.org/10.1007/s12192-008-0053-1
38. Zhang L, Lai E, Teodoro T, Volchuk A. GRP78, but Not Protein-disulfide Isomerase, Partially Reverses Hyperglycemia-induced Inhibition of Insulin Synthesis and Secretion in Pancreatic {beta}-Cells. J Biol Chem 2009; 284:5289-98; PMID:19103594; http://dx.doi.org/10.1074/jbc.M805477200
39. D'Hertog W, Overbergh L, Lage K, Ferreira GB, Maris M, Gysemans C, Flamez D, Cardozo AK, Van den Bergh G, Schoofs L, et al. Proteomics analysis of cytokine-induced dysfunction and death in insulin-producing INS-1E cells: new insights into the pathways involved. Mol Cell Proteomics 2007; 6:2180-99; PMID:17921177; http://dx.doi.org/10.1074/mcp.M700085-MCP200
40. Linssen MM, van Raalte DH, Toonen EJ, Alkema W, van der Zon GC, Dokter WH, Diamant M, Guigas B, Ouwens DM. Prednisolone-induced beta cell dysfunction is associated with impaired endoplasmic reticulum homeostasis in INS-1E cells. Cell Signal 2011; 23:1708-15; PMID:21689745; http://dx.doi.org/10.1016/j.cellsig.2011.06.002
41. Yagishita Y, Fukutomi T, Sugawara A, Kawamura H, Takahashi T, Pi J, Uruno A, Yamamoto M. Nrf2 protects pancreatic beta-cells from oxidative and nitrosative stress in diabetic model mice. Diabetes 2014; 63:605-18; PMID:24186865; http://dx.doi.org/10.2337/db13-0909
42. Ricordi C, Lacy PE, Finke EH, Olack BJ, Scharp DW. Automated method for isolation of human pancreatic islets. Diabetes 1988; 37:413-20; PMID:3288530; http://dx.doi.org/10.2337/diab.37.4.413
43. Mortz E, Krogh TN, Vorum H, Gorg A. Improved silver staining protocols for high sensitivity protein identification using matrix-assisted laser desorption/ionization-time of flight analysis. Proteomics 2001; 1:1359-63; PMID:11922595; http://dx.doi.org/10.1002/1615-9861(200111)1:11%3c1359::AID-PROT1359%3e3.0.CO;2-Q